AIP | Applied Physics Letters

Charge-induced reversible bending in nanoporous alumina-aluminum composite

Chuan Cheng and A. H. W. Ngan

Citation: Applied Physics Letters **102**, 213119 (2013); doi: 10.1063/1.4808212
View online: http://dx.doi.org/10.1063/1.4808212
View Table of Contents: http://scitation.aip.org/content/aip/journal/apl/102/21?ver=pdfcov
Published by the AIP Publishing

Charge-induced reversible bending in nanoporous alumina-aluminum composite

Chuan Cheng[a] and A. H. W. Ngan
Department of Mechanical Engineering, The University of Hong Kong, Pokfulam Road, Hong Kong, People's Republic of China

(Received 7 March 2013; accepted 16 May 2013; published online 31 May 2013)

Upon electrical charging, reversible bending was found in nanoporous anodic alumina-aluminum foil composites, as directly observed by an optical microscope and detected by *in situ* nanoindentation. The bending is thought to be the result of charge-induced surface stresses in the nanoporous alumina. The results suggest the possibility of a type of composite foil materials for applications as micro-scale actuators to transform electrical energy into mechanical energy. © *2013 AIP Publishing LLC*. [http://dx.doi.org/10.1063/1.4808212]

Electrical energy can be transformed into mechanical energy in materials such as piezoelectric ceramics,[1] electrostrictive polymers,[2] and carbon nanotubes,[3] as the dimensions of these materials can reversibly expand or contract upon cyclic electrical charging. Recently, charge-induced reversible straining was also observed in nanoporous noble metals,[4] such as Pt,[4] Au,[5] and Au-Pt alloys,[6] which are becoming a promising type of electrochemical actuators for potential applications such as artificial muscles.[7] The mechanism behind the charge-induced reversible straining in nanoporous metals is understood as follows.[4,6,8] When the nanoporous metal becomes an electrode within an electrochemical cell, an electrochemical double layer is formed along the metal surface, and due to the efficient electronic screening,[4] space charge is developed within the metal surface, which contributes to one half of the electrochemical double layer.[8] The modification of the free electron density at the metal surface can induce changes in the interatomic forces in the metal surface relative to the underlying bulk,[9] and as a consequence, surface stresses arise. To maintain mechanical equilibrium, stresses in the bulk are developed to balance the surface stresses,[4,10] and as a result, straining of the nanoporous metal takes place. The strain amplitude depends on the capacitance per weight of the actuator electrode, and the capacitance is proportional to the porous surface area and inversely proportional to the distance between the charges on the electrode and the counter charges in the electrolyte. Due to the extremely high surface-to-volume ratio in a nanoporous metal, high straining may be obtained.[4,7]

The above nano-porous metals are usually expensive noble metals Au, Pt, etc., made from costly processes such as de-alloying.[6,11] On the other hand, it is well known that relatively cheaper metals such as Al and Ti can be anodized to form a layer of nanoporous oxide, in which nano-sized pore channels grow vertically towards the metal substrate, and the pore size and porous pattern ordering can be conveniently controlled by the anodization conditions.[12–14] During anodization, electrochemical double layers are formed along the oxide/electrolyte (o/e) and metal/oxide (m/o) interfaces.[15] Due to the extremely high electric field intensity, on the order of 1 V/nm, within the scallop shaped oxide barrier layer[16] and the Cabrera-Mott potential barrier at the interfaces,[17] space charge may concentrate along the nanoporous oxide surface,[15] and as a result the interatomic bonding forces will be different from those in the oxide bulk. In contrary to nanoporous metals in which the space charge comes from free electrons,[4] the space charge in the oxide is mainly due to metal cations and oxygen anions. Upon the development of the charge-induced surface stress, the bi-layered nanoporous oxide–metal composite should deform. However, this type of actuation behavior has not been reported so far. In this work, a type of bi-layered composite of nanoporous anodic aluminum oxide (AAO) film supported on an Al metal foil was fabricated by anodization of the Al foil in an electrochemical cell, and the charge-induced reversible bending was investigated by optical microscopy and nanoindentation.

In order to directly observe the reversible bending of the AAO-Al foils upon electrical actuation, two types of *in situ* experiments were carried out. The first involved an optical microscope setup shown in Fig. 1(a). An electrochemical cell was placed on the sample stage of an optical microscope (Olympus Co.). A commercially pure Al foil (27 mm × 4.5 mm × 0.011 mm) acted as anode, where the foil thickness was measured in a LEO 1530 field-emission scanning electron microscope. A copper wire served as cathode. Both electrodes were connected to an external DC power supply (PAS 500-1.2, Kikusui Electronics Corp.). A CCD camera (CCD-IRIS, Color Video Camera, Sony Co.) was connected to the optical microscope by a microscope attachment (WV-9005, Matsushita Communication Industrial Co., LTD) in order to capture the magnified movement of the sample. The signal captured by the camera was channeled to a camera adapter (Model CMA-D7CE, Sony Co.) and was output onto a television monitor. Due to the projection, the total magnification of the sample on the monitor is about 1000 times. By using this setup, any significant movement of the free end of the sample, which was located at the focal point of the objective lens, can be seen on the monitor in real time. During the electrical actuation, the image on the monitor was recorded as videos by a digital camera placed in front.

The Al foil was mounted vertically onto the cell wall at one end, and the other end could freely move. The top edge

[a]Electronic mail: chuan.cheng.research@gmail.com.

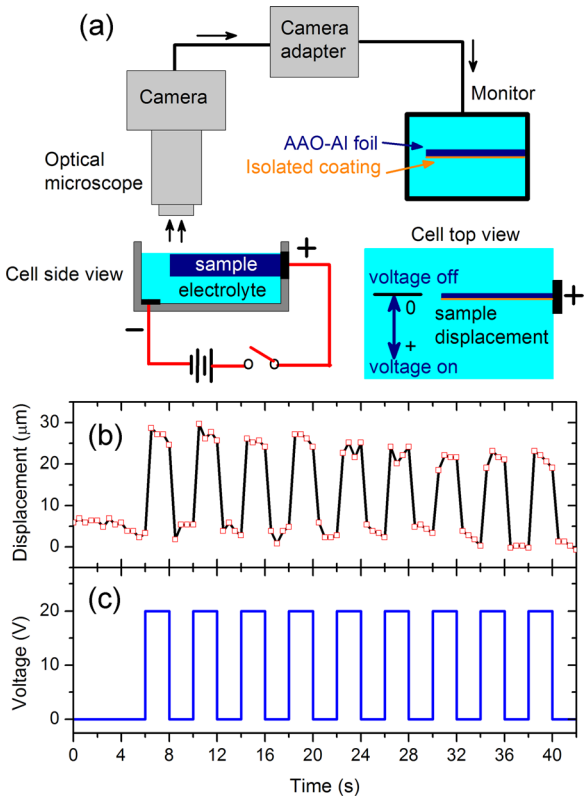

FIG. 1. (a) Schematic of an experimental setup for direct observation of the reversible bending in AAO-Al composite foil. (b) Displacement of the free end of the foil upon the cyclic electric actuation shown in (c). (enhanced online) Video 1 [URL: http://dx.doi.org/10.1063/1.4808212.1].

of the sample was parallel and very close to the electrolyte surface for the purpose of easy focus by the optical microscope on the free end of the sample. From the top view of the cell, the foil appeared edge-on, and one side of it was coated by a layer of insulating lacquer, so that only the other side can be anodized to form a layer of AAO. Before cyclic electric actuation, anodization of the Al foil was performed in the electrochemical cell under 20 V in 0.3M $H_2C_2O_4$ electrolyte at room temperature for about 30 s, so that a layer of AAO had already formed on the uncoated side of the Al foil. Upon cyclic electric actuation as shown in Fig. 1(c), the AAO-Al foil free end was found to move reversibly (see Video 1 link at Fig. 1). The displacement of the free end of the composite foil measured from the video at 0.5 s intervals is shown in Fig. 1(b). It can be seen that when the voltage was switched on, the displacement immediately increased to about 28.5 μm, which corresponds to the free end bending towards the coated side, as indicated by the double arrow in the top view in Fig. 1(a). This movement direction indicates that an expansive surface stress was developed within the layer of AAO on the uncoated side of the sample when the voltage was switched on, and this drove the sample to bend towards its coated side. After the bending movement, the displacement of the free end was found to about 25.5 $\pm$ 4.5 μm in the remaining of the 2 s with the voltage on, and once the voltage was switched off, the displacement immediately moved back to near its original position, indicating that the previous surface stress disappeared with the voltage switched off. This bending behavior is obviously reversible, and the same happens repeatedly in the following actuation circles, as shown in Fig. 1(b). See supplemental material for more evidence.[18]

In order to further investigate the reversible bending behavior, another experimental setup involving nanoindentation on the AAO-Al foils was designed as shown in Fig. 2(a). Before nanoindentation, an Al foil (1 in. in diameter, 1 mm in thickness) was pretreated as in Ref. 19. As shown in Fig. 2(a), another electrochemical cell was made to fit into the space between the sample stage and the transducer of the nanoindenter. A copper plate connected to an outside DC power supply was used to support the Al foil which acted as the anode. The copper plate was mounted into an insulated acrylic hot-mounting resin cylinder. The Al foil was attached to the top of copper plate using conductive epoxy, and then the circular rim between the Al foil and the cylinder was covered with a flexible rubber sleeve, so that only the central part of the Al foil was exposed to the electrolyte. A copper wire hoop was attached to the bottom of the cell and connected to the external power supply to serve as the cathode. The Al surface was about 2 mm below the free surface of the electrolyte. Anodization was conducted under 20 V in 0.2M $H_2C_2O_4$ electrolyte at room temperature. Nanoindentation was carried out on a Hysitron TriboScope nanoindenter (Hysitron, Inc.) mounted onto a ThermoMicroscopes scanning probe microscope in a load controlled manner. The indenter was a Berkovich tip designed for use in liquid (Hysitron, Inc.). The load function consisted of a load ramp at 100 μN/s followed by a 5 s holding time at the maximum load $P_{max} = 500$ μN and then a 5 s holding time at 10% P_{max} in the unloading stage. Although each nanoindentation period was set to be 20 s in the load function, in practice the nanoindenter would add 1s before loading and 3 s after unloading, so that the real indentation period was 24 s. All the results reported below

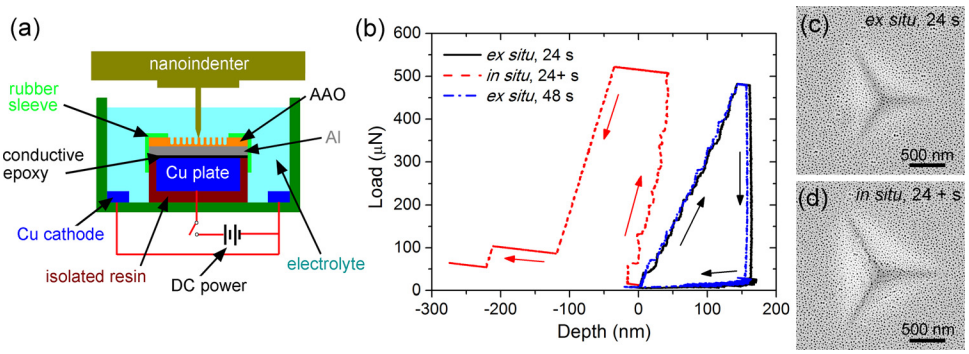

FIG. 2. (a) Schematic of an experimental setup for nanoindentation on AAO-Al composite foils. (b) Load against depth for *ex situ* and *in situ* nanoindentation. (c) and (d) SEM images of the corresponding *ex situ* (24 s) and *in situ* (24+ s) nanoindentation impressions, respectively.

were obtained from the AAO grown on the same (001) orientated Al grain, the crystallographic orientation of which was detected by electron back-scatter diffraction (EBSD) before anodization, so that the influence of substrate grain orientation was eliminated.[20]

The anodic voltage was cyclically switched. *Ex situ* nanoindentation with voltage off was first performed for one indentation period, and immediately afterwards, *in situ* nanoindentation with anodic voltage on was conducted on a fresh location ~4 μm away from the previous indent. Due to the AAO growth with anodic voltage on, the condition of the indented sample changes from one cyclic test to the next. Thus, to distinguish different indentation tests, these are labeled according to the cumulative anodization time, which is the sum of the time durations when the anodic voltage was turned on, from the beginning of the nanoindentation experiment. In a typical *ex situ* nanoindentation experiment, Fig. 2(b) (black curve) shows that, at the anodization time of 24 s, the depth first increased in the positive load, downward direction with load increasing, and then continuously increased during the holding at P_{max} due possibly to creep, and after that the depth almost kept the same as the indenter unloaded. Immediately after that, *in situ* nanoindentation with anodic voltage switched on was performed at the anodization time 24+ s, where "+" represents that the AAO was still growing during the indentation. As denoted by the red arrows in Fig. 2(b), the *in situ* depth only increased slightly at the loading stage, after that the depth continuously decreased towards the negative, upward direction during both holding and unloading stages, until reaching −275 nm at the end of indentation period. This indicates that the indenter tip has moved to a position 275 nm above its original position (depth = 0 nm). Immediately after that, *ex situ* nanoindentation with anodic voltage switched on was performed at the anodization time of 48 s (blue curve). Similar to that conducted *ex situ* at 24 s, the indentation depth also started to grow from zero with load increasing, which indicates that the indenter tip has returned to the original position after the voltage was switched off. Therefore, Fig. 2(b) shows that with anodic voltage turned on and off, the detected depth exhibited a reversible behavior, which indicates that the sample surface bent upward with voltage on and then returned to the initial flat state again with voltage switched off. Furthermore, as shown Fig. 2(c), the residual impression area (A_r) for *ex situ* nanoindentation at 24 s is about 0.71 μm^2. According to the shape function of the Berkovich tip ($A_r \approx 24.5h_r^2$), the calculated residual impression depth is about 170 nm, which is quite close to the residual depth detected in the load-depth curve in Fig. 2(b). However, for the *in situ* nanoindentation at 24+ s, the calculated residual depth obtained from its SEM impression area in Fig. 2(d) is about 215 nm, while the detected residual depth in Fig. 2(b) is about −275 nm which is nearly 500 nm less than the calculated value. The inconsistence indicates that the sample surface has bent by about 500 nm upward during the *in situ* nanoindentation.

Note that in order to carry out the *in situ* nanoindentation, the sample was attached on a Cu plate by conductive epoxy with its circular rim held down by a flexible rubber sleeve, and in this way the sample could not deform freely. Thus, the upward bending of the AAO-Al composite is restricted mechanically, and so the up-bending displacement shown in Fig. 2(b) develops slowly with time. But upon voltage switched off, the sample can quickly recover to the initial flat state because those mechanical constraints assist the recovery but act against up-bending. Also, volume expansion due to oxide formation from Al to Al_2O_3 cannot be the reason for the large and negative *in situ* displacements. Under the present anodization condition with average oxide growth rate of about 0.89 nm/s, the formed oxide thickness should be about 21 nm during one *in situ* nanoindentation period of 24 s. Typically, a unit volume of Al can only expand to about 1.18 times on oxidation, due to 30%–31% loss of Al to the electrolyte during anodization.[21] Thus, the net expanded thickness in the present case should be less than 3.2 nm, which is minute compared to the recorded up-bending displacement of ~500 nm. In addition, the compressive stresses within the AAO layer due to oxidation would not disappear when the voltage is switched off, because the oxidation is not reversed with the voltage switched off. Thus, they cannot contribute to the reversible bending behavior of the AAO-Al composite. See supplemental material for further discussion.[18]

The reasonable explanation for the detected reversible behavior, as shown in Figs. 1(b) and 2(b), is the charge-induced stress at the surface of the nanoporous oxide which forms and disappears with anodic voltage turned on and off. As schematically shown in Figs. 3(a) and 3(b), with anodic voltage turned off, the bi-layered AAO-Al composite is flat without charge-induced bending, while with voltage switched on, a type of charge-induced surface stress forms within the nanoporous AAO layer, causing the composite foil to bend away from the other side of the foil without AAO layer formation. As shown in Fig. 3(c), the applied anodization potential mainly drops across the barrier layer at the pores' bottom,[22] where the electric field intensity is much higher than other locations in the oxide. Due to the Cabrera-Mott potential barrier at the interfaces,[17] the space-charge from electrolyte anions (e.g., O^{2-}) and metal cations (e.g., Al^{3+}) will be mainly attracted by the electrical field at the o/e and m/o interfaces along the barrier layer. Interatomic forces along both interfaces of the scallop shaped barrier layer should be modified due to the charge concentration, and as a consequence, significant surface stresses should arise at the pore bottom region. These may cause the curvature of the U-shaped pore channels to expand, compared with the previous profile with voltage off (dashed line in Fig. 3(c)); macroscopically, the whole bi-layered composite will be bent upward as shown in Fig. 3(b). Note that the capacitance of the AAO layer will not increase with the AAO growing thicker and the total o/e surface area increasing, because the effective area for the attraction of charges is the surface area of the barrier layer at the bottom of the pore channels, which almost does not change after the anodization has reached a steady state, regardless of how thick the oxide structure above is. This is why the displacement shown in Fig. 1(b) is maintained in the same range with time increasing. This situation is different from the nanoporous metals, in which the capacitance increases with total surface area of the structure due to highly efficient electronic screening.[4] In addition, during up-bending, the nanopore channels will be slightly opened up, as if the structure is inhaling extra volume of the electrolyte.

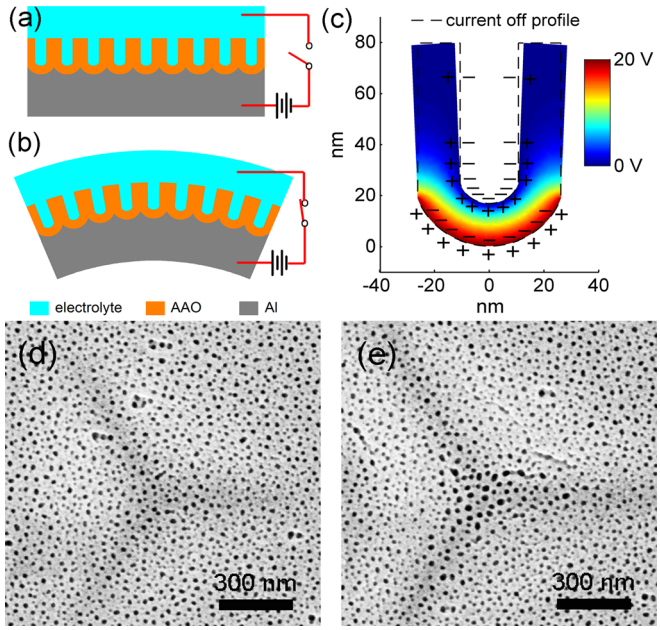

FIG. 3. Schematics of AAO-Al composite immersed into the electrolyte during (a) *ex situ*, and (b) *in situ* nanoindentation with anodic voltage off and on, respectively. (c) Expanded pore channel during *in situ* nanoindentation, relative to the *ex situ* pore channel profile with voltage off shown by the dashed lines. SEM images of normal and expanded pore mouths at the center of (d) *ex situ* and (e) *in situ* nanoindentation impressions obtained at the anodization time of 48 s and 48+ s, respectively.

During the opening up of the nanopores, if nanoindentation is conducted *in situ*, the enlarged nanopore mouths will be plastically deformed and cannot revert to their previous *ex situ* state, and so the enlarged sizes of the pore mouths will be left in the nanoindentation impression. This is verified by Figs. 3(d) and 3(e), which show that the pore size at the center of the *in situ* impression (Fig. 3(e)) is much larger than that in the *ex situ* impression (Fig. 3(d)), whereas the pore size in the *ex situ* case is similar within and outside the impression.

The present AAO-Al foils may be used as micro-scale actuators within an electrolyte environment under very low actuation voltages. However, the lifetime of the actuator is limited because the Al substrate is consumed with voltage switched on. This drawback may be overcome by switching the present electrolyte to a much weaker acidic electrolyte after formation of an AAO layer. For example, with an aqueous borate solution as electrolyte, only a thin layer of barrier-type oxide can be formed on the Al surface,[23] and if AAO is already present on the surface, the weak electrolyte cannot result in further growth of the pore channels, and thus the consumption of Al will be eliminated. Furthermore, like Al, a group of other metals including Ti, Nb, Ta, Zr, Hf, etc., can also form nanoporous oxide on their surface.[24] Similar reversible bending behavior may also happen in oxide-metal bi-layered foils made from these metals.

In conclusion, charge-induced reversible bending of bi-layered AAO-Al foil composites was directly observed *in situ* in an electrochemical cell by an optical microscope as well as nanoindentation setup upon cyclic electric actuations. The results here may open up opportunities for the development of a type of composite materials for micro-scale actuator applications to transform electrical energy into mechanical energy.

The authors acknowledge financial support from University Grants Committee (Project No. SEG-HKU06) of the Hong Kong Special Administration Region as well as the Kingboard Endowed Professorship.

[1]Q. Zhang, V. Bharti, and X. Zhao, Science **280**, 2101 (1998).
[2]R. H. Baughman, Synth. Met. **78**, 339 (1996).
[3]R. H. Baughman, C. Cui, A. A. Zakhidov, Z. Lqbal, J. N. Barisci, G. M. Spinks, G. G. Wallace, A. Mazzoldi, D. D. Rossi, A. G. Rinzler *et al.*, Science **284**, 1340 (1999).
[4]J. Weissmüller, R. N. Viswanath, D. Kramer, P. Zimmer, R. Würschum, and H. Gleiter, Science **300**, 312 (2003).
[5]E. Detsi, S. Punzhin, J. Rao, P. R. Onck, and J. T. M. De Hosson, ACS Nano **6**, 3734 (2012).
[6]H. J. Jin, X. L. Wang, S. Parida, K. Wang, M. Seo, and J. Weissmüller, Nano Lett. **10**, 187 (2010).
[7]R. H. Baughman, Science **300**, 268 (2003).
[8]H. J. Jin and J. Weissmüller, Adv. Eng. Mater. **12**, 714 (2010).
[9]H. Ibach, Surf. Sci. Rep. **29**, 195 (1997).
[10]J. Weissmüller and J. W. Cahn, Acta Mater. **45**, 1899 (1997).
[11]D. Kramer, R. N. Viswanath, and J. Weissmüller, Nano Lett. **4**, 793 (2004).
[12]H. Masuda and K. Fukuda, Science **268**, 1466 (1995).
[13]H. C. Sin, J. Dong, and M. Liu, Adv. Mater. **16**, 237 (2004).
[14]W. Lee, R. Ji, U. Gösele, and K. Nielsch, Nature Mater. **5**, 741 (2006).
[15]M. M. Lohrengel, Mater. Sci. Eng. R **11**, 243 (1993).
[16]J. E. Houser and K. R. Hebert, Nature Mater. **8**, 415 (2009).
[17]N. Cabrera and N. F. Mott, Rep. Prog. Phys. **12**, 163 (1949).
[18]See supplementary material at http://dx.doi.org/10.1063/1.4808212 for more discussion.
[19]C. Cheng, K. Y. Ng, and A. H. W. Ngan, AIP Adv. **1**, 042113 (2011).
[20]C. K. Y. Ng and A. H. W. Ngan, Chem. Mater. **23**, 5264 (2011).
[21]F. Li, L. Zhang, and R. M. Metzger, Chem. Mater. **10**, 2470 (1998).
[22]C. Cheng and A. H. W. Ngan, Electrochim. Acta **56**, 9998 (2011).
[23]P. Skeldon, K. Shimizu, G. E. Thompson, and G. C. Wood, Surf. Interface Anal. **5**, 247 (1983).
[24]Z. Su and W. Zhou, Adv. Mater. **20**, 3663 (2008).